Transp Porous Med (2012) 93:127–145
DOI 10.1007/s11242-012-9947-6

Anomalous Reactive Transport in the Framework of the Theory of Chromatography

Valentina Prigiobbe · Marc A. Hesse · Steven L. Bryant

Received: 28 September 2011 / Accepted: 23 January 2012 / Published online: 10 February 2012

Abstract The anomalous reactive transport considered here is the migration of contaminants through strongly sorbing permeable media without significant retardation. It has been observed in the case of heavy metals, organic compounds, and radionuclides, and it has critical implications on the spreading of contaminant plumes and on the design of remediation strategies. Even in the absence of the well-known fast migration pathways, associated with fractures and colloids, anomalous reactive transport arises in numerical simulations of reactive flow. It is due to the presence of highly pH-dependent adsorption and the broadening of the concentration front by hydrodynamic dispersion. This leads to the emergence of an isolated pulse or wave of a contaminant traveling at the average flow velocity ahead of the retarded main contamination front. This wave is considered anomalous because it is not predicted by the classical theory of chromatography, unlike the retardation of the main contamination front. In this study, we use the theory of chromatography to study a simple pH-dependent surface complexation model to derive the mathematical framework for the anomalous transport. We analyze the particular case of strontium (Sr^{2+}) transport and define the conditions under which the anomalous transport arises. We model incompressible one-dimensional (1D) flow through a reactive porous medium for a fluid containing four aqueous species: H^+, Sr^{2+}, Na^+, and Cl^-. The mathematical problem reduces to a strictly hyperbolic 2×2 system of conservation laws for effective anions and Sr^{2+}, coupled through a competitive Langmuir isotherm. One characteristic field is linearly degenerate while the other is not

V. Prigiobbe (✉) · S. L. Bryant
Department of Petroleum and Geosystems Engineering, University of Texas at Austin,
1 University Station, Austin, TX 78712, USA
e-mail: valentina.prigiobbe@mail.utexas.edu

M. A. Hesse
Department of Geological Sciences, University of Texas at Austin, 1 University Station, Austin,
TX 78712, USA

M. A. Hesse · S. L. Bryant
Institute for Computational Engineering and Sciences, University of Texas at Austin,
1 University Station, Austin, TX 78712, USA

genuinely nonlinear due to an inflection point in the pH-dependent isotherm. We present the complete set of analytical solutions to the Riemann problem, consisting of only three combinations of a slow wave comprising either a rarefaction, a shock, or a shock–rarefaction with fast wave comprising only a contact discontinuity. Highly resolved numerical solutions at large Péclet numbers show excellent agreement with the analytic solutions in the hyperbolic limit. In the Riemann problem, the anomalous wave forms only if: hydrodynamic dispersion is present, the slow wave crosses the inflection locus, and the effective anion concentration increases along the fast path.

Keywords Anomalous transport · Theory of chromatography · Hyperbolic systems · Reactive transport · Strontium

1 Introduction

The term *anomalous reactive transport* is used here to refer to the migration of contaminants through strongly sorbing permeable media without significant retardation and in contrast to the use of the term anomalous solute transport in the context of non-Fickian diffusion (Scher et al. 2002; Berkowitz et al. 2006) or multiple-rate mass-transfer (Haggerty and Gorelick 1995). If anomalous reactive transport is not anticipated, the migration distance of highly toxic compounds such as heavy metals, organic substances, and radionuclides in groundwater will be underestimated and field observations could be interpreted incorrectly.

Many radionuclides have a strong affinity to adsorb to soils and their migration velocity is therefore expected to be significantly less than the average groundwater velocity. Faster radionuclide migration than expected from the adsorption characteristics of the soil has been observed upon leakage of radioactive solutions into the groundwater at some of the DOE facilities in the USA [e.g., Hanford (WA), Oak Ridge (TN), Savannah River (SC), and Radioactive Waste Management Complex (ID)]. Liquid wastes of variable composition and containing fission products such as ^{90}Sr, ^{137}Cs, ^{60}Co, and U(VI) contaminated the nearby aquifers and high levels of radioactivity were measured at the observation wells (Saunders and Toran 1995; Spalding and Spalding 2001; Greskowiak et al. 2011). One of the most common radionuclides measured at these locations is ^{90}Sr, which is considered to be the most critical radioactive isotope in the environment, by the US Environmental Protection Agency (US EPA 2011, Wieland et al. 2008), because its chemical similarity with Ca^{2+} leads to its deposition in human bone and in blood-forming tissue increasing the long-term risk of leukemia (US EPA 2011).

In the particular case of the leakage event detected at Oak Ridge, the concentration of ^{90}Sr in the underground aquifer indicated that ^{90}Sr migrated much further than predicted by transport models based on simple retardation factor which underestimated the travel distance (Saunders and Toran 1995). Beyond the well-known fast transport processes due to fractures and colloids, competitive adsorption associated to the high reactivity of the permeable media was also considered responsible for that fast migration (Toran et al. 1998; Bryant et al. 2000). Numerical simulations of this event by Toran et al. (1998) and Bryant et al. (Bryant et al. 2000) applied coupled transport and surface complexation models and argue that the combination of a large hydrodynamic dispersion with the nonlinearity of the competitive adsorption gives rise to Sr^{2+} concentration profiles characterized by a retarded front and a pulse traveling at the average flow velocity. Historically hydrodynamic dispersion has been regarded as a second-order effect in the development of reaction fronts (Rhee et al. 1971), which only smooths waves predicted by the theory of chromatography, but does not change

their speed, much less create new waves. This unretarded pulse is therefore not predicted by the classical theory of chromatography (Rhee et al. 1989) and considered anomalous in that mathematical framework. This phenomenon was observed both in numerical simulations and in field measurements, although other explanations are possible in the latter case.

Here, we focus on the analysis of this phenomenon in numerical simulations, in particular, on the case of the pH-dependent sorption required for the anomalous transport, which has never been analyzed rigorously with of the theory of chromatography. The chromatographic analysis is necessary to provide the mathematical framework against which the fast moving pulse can be compared and identified as anomalous. This analysis is carried out in this article, where we solve the Riemann problem (i.e., initial data are given by two constant states separated by a single discontinuity) for the 2×2 nonlinear system of conservation laws describing 1D transport of strontium and protons through a reactive porous medium made of hydrous ferric oxide (HFO). In the absence of hydrodynamic dispersion, the system is strictly hyperbolic with characteristic fields either not genuinely nonlinear or linearly degenerate, and we determine the complete set of admissible solutions and compare them with numerical simulations.

The article consists of six sections. In Sect. 2, we describe the geochemical model, i.e., the reactions in the solution and at the solid–liquid interface. In Sect. 3, we give the governing equations of the transport model; in Sect. 4, we solve the Riemann problem in the limit of negligible hydrodynamic dispersion (theory of chromatography), and in Sect. 5, we give the complete set of admissible solutions to the Riemann problem. In Sect. 6, we show that hydrodynamic dispersion introduces an anomalous additional wave that is superimposed on the chromatographic solution, and we determine the conditions under which the anomalous transport occurs.

2 Geochemical Model

We study the aqueous system containing H^+, Sr^{2+}, Na^+, and Cl^- and a solid coated with HFO, which is an iron oxide with a poorly ordered crystalline structure containing hydroxyl groups and water molecules (Das et al. 2011). We describe the surface of HFO following CD-MUSIC model (Hiemstra et al. 1989, 2004; Hiemstra and Van Riemsdijk 1996) in which the surface reactive sites are defined on the base of the crystallography of the mineral. Following van Beinum et al. (2005) and considering the analogy between HFO and goethite, we assumed for HFO the same set of surface sites of goethite. There are three types of sites either coordinated singly ($FeOH^{-1/2}$), doubly (Fe_2OH^0), or triply ($Fe_3O^{-1/2}$) and we wrote the chemical reactions occurring in a CO_2-free solution as:

$$\equiv XO^{-1/2} + H^+ \longleftrightarrow \equiv XOH^{+1/2}, \tag{1}$$

$$\equiv XO^{-1/2} + Sr^{2+} \longleftrightarrow \equiv XO^{-1/2} - Sr^{2+}, \tag{2}$$

$$\equiv XO^{-1/2} + Na^+ \longleftrightarrow \equiv XO^{-1/2} - Na^+, \tag{3}$$

$$\equiv XOH^{+1/2} + Cl^- \longleftrightarrow \equiv XOH^{+1/2} - Cl^-, \tag{4}$$

where $\equiv XO^{-1/2}$ corresponds to a singly or a triply coordinated site. Neglecting the electrostatic term of the effective equilibrium constant that accounts for the development of the surface charges upon adsorption, the effective equilibrium constants equal the intrinsic equilibrium constants and for the above reactions they are given as:

$$K_{\mathrm{H}} = \frac{\{\equiv \mathrm{XOH}^{+1/2}\}}{C_{\mathrm{H}}\{\equiv XO^{-1/2}\}} = 10^{8.73}, \tag{5}$$

$$K_{\mathrm{Sr}} = \frac{\{\equiv \mathrm{XO}^{-1/2} - \mathrm{Sr}^{2+}\}}{C_{\mathrm{Sr}}\{\equiv \mathrm{XO}^{-1/2}\}} = 10^{4.47}, \tag{6}$$

$$K_{\mathrm{Na}} = \frac{\{\equiv \mathrm{XO}^{-1/2} - \mathrm{Na}^{+}\}}{C_{\mathrm{Na}}\{\equiv \mathrm{XO}^{-1/2}\}} = 10^{-1.5}, \tag{7}$$

$$K_{\mathrm{Cl}} = \frac{\{\equiv \mathrm{XOH}^{+1/2} - \mathrm{Cl}^{-}\}}{C_{\mathrm{Cl}}\{\equiv \mathrm{XOH}^{+1/2}\}} = 10^{-1}, \tag{8}$$

where C_i corresponds to the concentrations of the subscripted species, (mol kg^{-1}), and the equilibrium constants are given at 25°C in kg mol^{-1} (Hiemstra et al. 2004; van Beinum et al. 2005). The adsorption of Na^+ and Cl^- is negligible in comparison to the adsorption of H^+ and Sr^{2+}, therefore, we assume that Na^+ and Cl^- are conservative and introduce the effective anion concentration in the fluid

$$C_{\mathrm{a}} = C_{\mathrm{Cl}} - C_{\mathrm{Na}}, \tag{9}$$

and the simplified site balance equation

$$Z_{\mathrm{t}} = \{\equiv \mathrm{XOH}^{-1/2}\} + \{\equiv \mathrm{XOH}^{+1/2}\} + \{\equiv \mathrm{XOH}^{-1/2} - \mathrm{Sr}^{2+}\}, \tag{10}$$

where Z_t is the total concentration of the reactive surface site (mol kg^{-1}).

We combine Eqs. 5, 6, and 10 and we derive the adsorbed concentration of H^+, Z_H, and Sr^{2+}, Z_{Sr}, on the HFO surface (mol kg^{-1}), which are classical competitive Langmuir isotherms (Rhee et al. 1989), given by,

$$Z_{\mathrm{H}} = \frac{C_{\mathrm{H}} K_{\mathrm{H}} Z_{\mathrm{t}}}{1 + C_{\mathrm{H}} K_{\mathrm{H}} + C_{\mathrm{Sr}} K_{\mathrm{Sr}}}, \tag{11}$$

$$Z_{\mathrm{Sr}} = \frac{C_{\mathrm{Sr}} K_{\mathrm{Sr}} Z_{\mathrm{t}}}{1 + C_{\mathrm{H}} K_{\mathrm{H}} + C_{\mathrm{Sr}} K_{\mathrm{Sr}}}. \tag{12}$$

Our analysis deviates from previous chromatographic theory applied to natural systems (Pope et al. 1978; Charbeneau 1981, 1988; Valocchi et al. 1981; Appelo 1996; Appelo et al. 1993), because in surface complexation models protons are competing for sites, as well. This leads to characteristic pH dependence and therefore the hydrolysis of water

$$\mathrm{H_2O} \longleftrightarrow \mathrm{OH}^{-} + \mathrm{H}^{+}, \tag{13}$$

has to be considered. Assuming the activity of water equal to the unity, the equilibrium constant for Eq. 13 at 25°C is given by,

$$K_{\mathrm{w}} = C_{\mathrm{OH}} C_{\mathrm{H}} = 10^{-14}. \tag{14}$$

In this analysis, we assume the aqueous phase is charge balanced and the electroneutrality condition is given by,

$$C_{\mathrm{OH}} + C_{\mathrm{a}} = C_{\mathrm{H}} + 2C_{\mathrm{Sr}}, \tag{15}$$

where we also neglect the charge developed at the solid–liquid interface upon adsorption. By combining Eqs. 14 and 15, we derive an algebraic equation for the concentration of H^+

$$C_{\mathrm{H}} = \frac{-(2C_{\mathrm{Sr}} - C_{\mathrm{a}}) \pm \sqrt{(2C_{\mathrm{Sr}} - C_{\mathrm{a}})^2 + 4K_{\mathrm{w}}}}{2}, \tag{16}$$

which gives a physically admissible value if the positive root is chosen. The dissociation of water adds a strong additional nonlinearity and commonly leads to pH transients in chromatographic columns (Bankston et al. 2010; Dattolo et al. 2010; Pabst and Carta 2007).

Substituting Eqs. 9 and 16 into Eqs. 11 and 12, the adsorption isotherms for H^+ and Sr^{2+} become

$$Z_{\mathrm{H}} = \frac{0.5\left[-(2C_{\mathrm{Sr}} - C_{\mathrm{a}}) + \sqrt{\Delta}\right] K_{\mathrm{H}} Z_{\mathrm{t}}}{1 + 0.5\left[-(2C_{\mathrm{Sr}} - C_{\mathrm{a}}) + \sqrt{\Delta}\right] K_{\mathrm{H}} + C_{\mathrm{Sr}} K_{\mathrm{Sr}}}, \tag{17}$$

$$Z_{\mathrm{Sr}} = \frac{C_{\mathrm{Sr}} K_{\mathrm{Sr}} Z_{\mathrm{t}}}{1 + 0.5\left[-(2C_{\mathrm{Sr}} - C_{\mathrm{a}}) + \sqrt{\Delta}\right] K_{\mathrm{H}} + C_{\mathrm{Sr}} K_{\mathrm{Sr}}}, \tag{18}$$

where

$$\Delta = (2C_{\mathrm{Sr}} - C_{\mathrm{a}})^2 + 4K_{\mathrm{w}} > 0.$$

Figure 1 shows Z_{Sr} as a function of C_{a} and C_{Sr} and the cross section with increasing C_{Sr} and at constant C_{a} in Fig. 1b illustrates the sigmoidal shape of the isotherm characterized by an inflection point (Glueckauf 1947), which separates it into two parts, a convex part and a concave part with the latter resembling a standard Langmuir isotherm. The C_{Sr} of the inflection point increases monotonically with C_{a} on the C_{a}–C_{Sr} plane shown in Fig. 1d. This *inflection locus* is associated to the maxima of one of the two eigenvalues of the transport model and it is important both in the development of the chromatographic theory as well as for the formation of the anomalous wave. Figure 1c shows a cross section of the adsorption isotherm surface at constant C_{Sr} and it corresponds to the typical adsorption edge of sorbed metals with increasing pH (Zhu and Schwartz 2011). The contour lines of the pH on the C_{a}–C_{Sr} plane are shown in Fig. 1d. This plane is divided in two parts, a region below the inflection locus where the pH is acidic and the adsorption is negligible and another above it where the pH is alkaline and the adsorption is large.

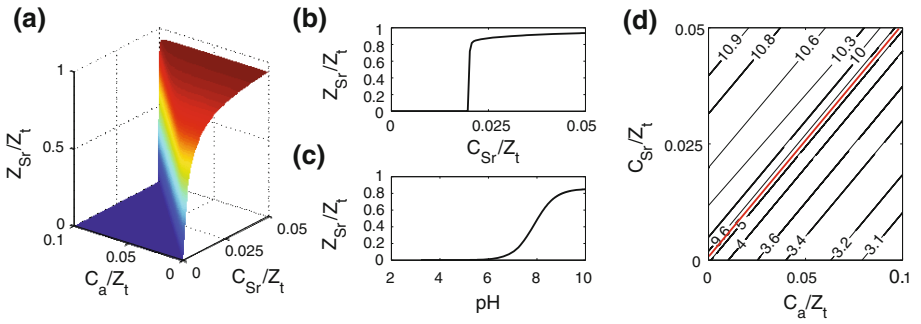

Fig. 1 Competitive adsorption isotherm (Z_{Sr}) given in Eq. 18 and the contour lines of pH calculated through Eq. 16. **a** Z_{Sr} as a function of C_{a} and C_{Sr}; **b** Z_{Sr} vs. C_{Sr} at $C_{\mathrm{a}} = 4 \cdot 10^{-4}$ m; **c** Z_{Sr} vs. pH at $C_{\mathrm{Sr}} = 10^{-4}$ m; and **d** contour lines of pH and the inflection locus indicated in *red*. All the concentrations except for the pH have been divided by the total concentration of reactive sites, Z_{t}

3 Mathematical Model

3.1 Governing Equations

We study incompressible, 1D, isothermal reactive transport of a four component (H^+, Sr^{2+}, Na^+, and Cl^-) aqueous system through a homogeneous porous medium under the assumption of local chemical equilibrium (Rhee and Amundson 1972; Knapp 1989). The transport equations are given by two partial differential equations

$$\frac{\partial}{\partial t}(C_{\mathrm{Sr}} + \phi Z_{\mathrm{Sr}}) + v\frac{\partial C_{\mathrm{Sr}}}{\partial x} - D\frac{\partial^2 C_{\mathrm{Sr}}}{\partial x^2} = 0, \tag{19}$$

$$\frac{\partial C_{\mathrm{a}}}{\partial t} + v\frac{\partial C_{\mathrm{a}}}{\partial x} - D\frac{\partial^2 C_{\mathrm{a}}}{\partial x^2} = 0, \tag{20}$$

on $-\infty < x < \infty$ and for $t > 0$, and the algebraic Eq. 16 for C_{H} in terms of C_{Sr} and C_{a} (Glueckauf 1947), where D is the hydrodynamic dispersion ($\mathrm{m^2\,s^{-1}}$); v is the interstitial fluid velocity ($\mathrm{m\,s^{-1}}$); and ϕ the dimensionless ratio of solid to fluid volume defined as $\phi = (1-\varepsilon)/\varepsilon$ with ε the porosity (–). This system is similar to that considered by Charbeneau (1981) and Lake et al. (2002), but the isotherm, Eq. 18, is different.

Using the total number of sites, Z_{t}, the characteristic length of the system, L, and the time for a conservative tracer to traverse the system by advection, $t_{\mathrm{a}} = L/v$, we introduce the dimensionless variables

$$c_{\mathrm{s}} = \frac{C_{\mathrm{Sr}}}{Z_{\mathrm{t}}},\ c_{\mathrm{a}} = \frac{C_{\mathrm{a}}}{Z_{\mathrm{t}}},\ z_{\mathrm{s}} = \frac{Z_{\mathrm{Sr}}}{Z_{\mathrm{t}}},\ \xi = \frac{x}{L},\ \tau = \frac{t}{t_{\mathrm{a}}} = \frac{tv}{L}.$$

The dimensionless governing equations of the transport model are given by

$$\frac{\partial}{\partial \tau}(c_{\mathrm{s}} + \phi z_{\mathrm{s}}) + \frac{\partial c_{\mathrm{s}}}{\partial \xi} - \frac{1}{Pe}\frac{\partial^2 c_{\mathrm{s}}}{\partial \xi^2} = 0, \tag{21}$$

$$\frac{\partial c_{\mathrm{a}}}{\partial \tau} + \frac{\partial c_{\mathrm{a}}}{\partial \xi} - \frac{1}{Pe}\frac{\partial^2 c_{\mathrm{a}}}{\partial \xi^2} = 0, \tag{22}$$

where Pe is the Péclet number, i.e., the ratio of the advective, t_{a}, and the diffusive, $t_{\mathrm{d}} = L^2/D$, timescales

$$Pe = \frac{t_{\mathrm{a}}}{t_{\mathrm{d}}} = \frac{vL}{D}. \tag{23}$$

In the limit of large Pe, the hydrodynamic dispersion is negligible and the resulting hyperbolic system of equations can be therefore analyzed by the theory of chromatography.

4 The Theory of Chromatography and Hyperbolic Conservation Laws

In the limit of $Pe \gg 1$, the governing equations are given by the following quasi-linear hyperbolic system

$$\frac{\partial \mathbf{a}(\mathbf{c})}{\partial \tau} + \frac{\partial \mathbf{c}}{\partial \xi} = 0, \quad \text{on} \quad -\infty < \xi < \infty,\ \tau > 0, \tag{24}$$

where $\mathbf{c} = (c_{\mathrm{s}}, c_{\mathrm{a}})$ is the vector of unknowns and $\mathbf{a}(\mathbf{c})$ is the accumulation term given by

$$\mathbf{a}(\mathbf{c}) = \mathbf{c} + \phi \mathbf{z}(\mathbf{c}), \tag{25}$$

where $\mathbf{z} = (z_s(\mathbf{c}), 0)$. We study the Riemann problem that considers the initial data given by a constant left-state, $\mathbf{c}_\mathrm{l}$, separated by a single discontinuity from the constant right-state, $\mathbf{c}_\mathrm{r}$,

$$\mathbf{c}(x, 0) = \begin{cases} \mathbf{c}_\mathrm{l} \text{ if } \xi < 0, \\ \mathbf{c}_\mathrm{r} \text{ if } \xi > 0. \end{cases} \tag{26}$$

The Riemann problem is of fundamental importance in the construction of the solution of hyperbolic systems of conservation laws and, in practical applications, it is useful to interpret experimental results, e.g., column-flood experiments.

The Riemann problem is invariant under an uniform stretching transformation of the independent variables ($\bar{x} = e^{\alpha} x, \bar{t} = e^{\alpha} t$) (Cantwell 2002), so that we seek a self-similar solution in the similarity variable $\eta := \xi/\tau$. The similarity transformation reduces the system of partial differential equations (eqs. 21 and 22) to the following system of ordinary differential equations

$$\left(\mathbf{A} - \frac{1}{\eta}\mathbf{I}\right)\frac{\mathrm{d}\mathbf{c}}{\mathrm{d}\eta} = 0, \tag{27}$$

where $\mathbf{A}$ is the Jacobian matrix of the system

$$\mathbf{A} = \nabla_\mathrm{c}\mathbf{a} = \mathbf{I} + \phi\nabla_\mathrm{c}\mathbf{z}. \tag{28}$$

The solution to the Riemann problem generally consists of a sequence of waves, each one propagating at a distinct but steady speed represented by the similarity variable. Below, we show that the system is strictly hyperbolic, and therefore the solution consists of two waves, $\mathscr{W}_1$ (slow wave) and $\mathscr{W}_2$ (fast wave), connecting three constant states, $\mathbf{c}_\mathrm{l}$ (left), $\mathbf{c}_\mathrm{m}$ (middle), and $\mathbf{c}_\mathrm{r}$ (right)

$$\mathbf{c}_\mathrm{l} \xrightarrow{\mathscr{W}_1} \mathbf{c}_\mathrm{m} \xrightarrow{\mathscr{W}_2} \mathbf{c}_\mathrm{r}. \tag{29}$$

The weak solution to the Riemann problem therefore consists of determining the nature and the speed of the two waves as well as the intermediate composition, $\mathbf{c}_\mathrm{m}$. The constant states trivially satisfy Eq. 27, because $\mathrm{d}\mathbf{c}/\mathrm{d}\eta = 0$. The waves connecting these constant states can either be continuous or discontinuous variations in composition that can be represented as paths in the composition space. The composition paths representing continuous variations are the integral curves of the eigenvalue problem associated with Eq. 27. The composition paths of the discontinuous variations, shock curves, are given by a system of nonlinear algebraic equations arising from mass conservation.

4.1 Hodograph Plane and Composition Paths

The solution to quasi-linear 2×2 system of equations is constructed and displayed in the space of the dependent variables also called state space or hodograph plane, the latter is most commonly used in the theory of chromatography and hyperbolic conservation laws. In reactive transport problems, the dependent variables are the compositions and therefore the hodograph plane also referred to as composition space (Helfferich and Klein 1970; Pope et al. 1978; Lake et al. 2002; Orr 2007).

4.1.1 Integral Curves

The composition paths of the admissible continuous variations are determined by the eigenvalue problem in Eq. 27 rewritten as

$$(\mathbf{A} - \sigma \mathbf{I})\mathbf{r} = 0, \tag{30}$$

where the eigenvalues, $\sigma = 1/\eta = \tau/\xi$, represent the inverse of the velocity, $\sigma = 1/v$, or the retardation of a composition and the eigenvectors, $\mathbf{r} = \mathrm{d}\mathbf{c}/\mathrm{d}\eta$, give the admissible continuous compositional variations. In the theory of hyperbolic conservation laws, the interpretation of the eigenvalue is usually the velocity of the propagation; whereas here it is the retardation, σ. The retardation arises because the nonlinearity is in the accumulation term instead of in the flux term (Rhee et al. 1989). The eigenvalues are the roots of the characteristic polynomial,

$$P(\sigma) = (1 - \sigma)\left(1 + \phi \frac{\partial z_\mathrm{s}}{\partial c_\mathrm{s}} - \sigma\right) = 0, \tag{31}$$

and are given by

$$\sigma_1 = 1 + \phi \frac{\partial z_\mathrm{s}}{\partial c_\mathrm{s}}, \tag{32a}$$

$$\sigma_2 = 1. \tag{32b}$$

The eigenvalues have been numbered in decreasing order so that the ordering of the waves in Eq. 29 from slow to fast is maintained. The strontium adsorption isotherm, z_s, is a monotonically increasing function of c_s (see Fig. 1a, b), so that $\sigma_2 < \sigma_1$. Figure 2a reports the contour lines of σ_1 on the c_a–c_s plane. The magnitude of σ_1 changes with the concentrations and is proportional to the slope of the strontium isotherm with a maximum in the vicinity of the inflection locus, as shown in Fig. 2b. While σ_2 is constant. The eigenvalues are real, positive, and distinct and hence the system is strictly hyperbolic (Lax 1957; Liu 1974; Ancona and Marson 2001). Consequently, there are two real and linearly independent eigenvectors given by

$$\mathbf{r}_1 = \begin{pmatrix} \frac{\mathrm{d}c_\mathrm{s}}{\mathrm{d}\eta} \\ \frac{\mathrm{d}c_\mathrm{a}}{\mathrm{d}\eta} \end{pmatrix} = \begin{pmatrix} 1 \\ 0 \end{pmatrix}, \tag{33a}$$

$$\mathbf{r}_2 = \begin{pmatrix} \frac{\mathrm{d}c_\mathrm{s}}{\mathrm{d}\eta} \\ \frac{\mathrm{d}c_\mathrm{a}}{\mathrm{d}\eta} \end{pmatrix} = \begin{pmatrix} \frac{\partial z_\mathrm{s}}{\partial c_\mathrm{a}} \\ -\frac{\partial z_\mathrm{s}}{\partial c_\mathrm{s}} \end{pmatrix}. \tag{33b}$$

The composition path of the $\mathscr{W}_i$ wave in the hodograph plane is obtained integrating the set of autonomous differential equations represented by $\mathbf{r}_i$ and therefore called the ith integral curves

$$\mathbf{c}_i(\mathbf{c}_0, \eta) = \mathbf{c}_0 + \int_0^\eta \mathbf{r}_i \, \mathrm{d}\eta'. \tag{34}$$

We will refer to the integral curves of $\mathbf{r}_1$ as the slow paths, $\mathscr{I}_1(\mathbf{c}_0)$, and those of $\mathbf{r}_2$ as the fast paths, $\mathscr{I}_2(\mathbf{c}_0)$. Along the slow paths the integration is trivial, because the anion concentration, c_a, is constant, so that they form a set of straight vertical lines in the hodograph plane as shown in Fig. 2c. Unlike problems in classical chromatography (Rhee et al. 1989; Lake et al. 2002), the fast paths here are not straight lines and Eq. 34 have to be integrated numerically. The fast paths, shown in Fig. 2c, are divided into two sets by a separatrix, shown to be the inflection locus below. The fast paths below the separatrix in the lower-right half

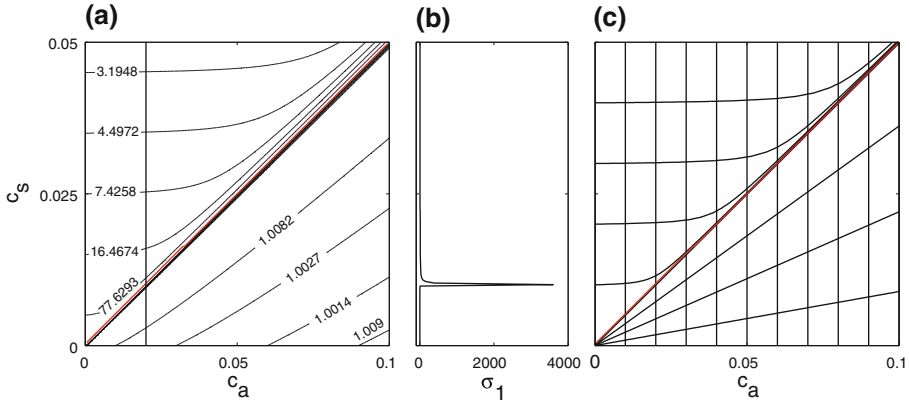

Fig. 2 The eigenvalues, the eigenvectors, and the inflection locus. **a** Contour lines of the eigenvalue σ_1 and the inflection locus indicated in *red*; **b** profile of σ_1 at $c_a = 0.2$ as indicated by the *black vertical line* in **a**; **c** hodograph plane and the inflection locus indicated in *red*

of the hodograph plane form rays from the origin similarly to those discussed by Lake et al. (2002). Far from the separatrix, the fast paths above the separatrix are horizontal but approach it asymptotically for large c_a. This complex pattern of the fast paths is due to the shape of the strontium isotherm. For a simpler system, Lake et al. (2002) have shown that $\mathbf{r}_2$ requires that the total differential of the adsorbed strontium concentration is conserved, i.e.,

$$\frac{dz_s}{d\eta} = \frac{\partial z_s}{\partial c_s}\frac{dc_s}{d\eta} + \frac{\partial z_s}{\partial c_a}\frac{dc_a}{d\eta} = 0. \tag{35}$$

The adsorbed strontium concentration is therefore constant along the fast path, which are given by the contour lines of the strontium isotherm, z_s, and the separatrix that divides them into two sets is the inflection locus of the isotherm.

4.1.2 Shock Curves or Hugoniot Loci

The composition paths and speeds of the admissible discontinuous variations connecting two compositions $\mathbf{c}_+$ and $\mathbf{c}_-$ are determined by the Rankine–Hugoniot jump condition

$$\tilde{\sigma}(\mathbf{c}_+; \mathbf{c}_-) = \frac{\mathbf{a}(\mathbf{c}_+) - \mathbf{a}(\mathbf{c}_-)}{\mathbf{c}_+ - \mathbf{c}_-} = 1 + \phi\frac{\mathbf{z}(\mathbf{c}_+) - \mathbf{z}(\mathbf{c}_-)}{\mathbf{c}_+ - \mathbf{c}_-}, \tag{36}$$

where $\tilde{\sigma}$ is the retardation of the discontinuity (Rhee et al. 1989). Again the retardation arises, instead of the velocity, because the nonlinearity is in the accumulation term instead of in the flux term. Given a composition $\mathbf{c}_-$, there are two equations for the three unknowns: $\tilde{\sigma}$ and the two components of $\mathbf{c}_+$. The jump condition therefore defines two sets of composition paths, referred to as the shock curves or Hugoniot loci, $\mathscr{H}_i(\mathbf{c}_-)$, which in general do not coincide with the integral curves defined in Sect. 4.1.1. Lax (1957) showed that the integral curves, $\mathscr{I}_i(\mathbf{c}_0)$, and the Hugoniot loci, $\mathscr{H}_i(\mathbf{c}_0)$, through any point $\mathbf{c}_0$ in composition space, are tangent to each other and have the same curvature. This implies that the first set of integral curves, $\mathscr{I}_1$, coincides with the first set of the Hugoniot loci, $\mathscr{H}_1$, because both are straight lines. The jump condition for $\mathscr{H}_2$ is given by the following equations

$$\tilde{\sigma} = 1 + \phi \frac{[z_s]}{[c_s]}, \tag{37a}$$

$$\tilde{\sigma} = 1, \tag{37b}$$

where the brackets indicate the difference between the two states connected by the discontinuity. The jump condition therefore requires that the change in the adsorbed strontium concentration across the discontinuity is zero, $[z_s] = 0$. The adsorbed strontium concentration along $\mathscr{H}_2$ is therefore constant, so that $\mathscr{H}_2$ is given by the contour lines of z_s and hence $\mathscr{H}_2$ is identical to $\mathscr{I}_2$.

Despite the complex nonlinear composition paths, both sets of shock and integral curves are identical and Eq. 24 is a system of Temple-class (Temple 1983). This greatly simplifies the construction and the presentation of the solution, because a unique set of fast and slow paths exists along which both continuous and discontinuous variations can be constructed.

5 Structure of the Solution

The theory of strictly hyperbolic systems was compiled by Lax (1957) for systems whose characteristic fields are either genuinely nonlinear or linearly degenerate. The theory of Lax was extended by Liu (1974) to find the Riemann solution of systems with nongenuinely nonlinear fields. In this article, we use this theory with the recent results by Ancona and Marson (2001) to describe the admissible solution structure and the complete set of solutions to the Riemann problem of the 1D reactive transport problem defined in Sect. 3.

For a 2×2 strictly hyperbolic system the solution to the Riemann problem consists of three constant states $\mathbf{c}_l$, $\mathbf{c}_m$, and $\mathbf{c}_r$ connected by a slow and a fast wave (Eq. 29). Because the system is Temple-class, both continuous and discontinuous waves lie along the composition paths defined on the hodograph plane (Fig. 2c) and the intersection of the composition paths defines the intermediate composition, $\mathbf{c}_m$. In this case, the solution along the fast path is linearly degenerate, $\sigma_2 = 1$, so that the fast wave, $\mathscr{W}_2$, is always a contact discontinuity, denoted by $\mathscr{C}_2$ (LeVeque 2008). This implies that $\mathbf{c}_l$ is always connected to $\mathbf{c}_m$ along the slow path and $\mathbf{c}_m$ to $\mathbf{c}_r$ through the fast path, so that

$$\mathbf{c}_l \xrightarrow{\mathscr{W}_1} \mathbf{c}_m \xrightarrow{\mathscr{C}_2} \mathbf{c}_r. \tag{38}$$

The structure of the solution along the slow path can be interpreted in terms of the shape of the isotherm. When the adsorption isotherm is a convex function such as in the case of the Langmuir isotherm, $\mathscr{W}_1$ can only be either a shock or a rarefaction (Mazzotti 2006); whereas when the adsorption isotherm is sigmoidal as in the present case (Fig. 1b), $\mathscr{W}_1$ may be composed of both a shock and a rarefaction (Liu 1974). The inflection point of the isotherm corresponds to the maximum of σ_1 along the slow path (Fig. 2b) where

$$\nabla \sigma_1(\mathbf{c}) \cdot \mathbf{r}_1(\mathbf{c}) = 0. \tag{39}$$

The problem is therefore not genuinely nonlinear in the sense of Lax (Lax 1957), and the slow wave, $\mathscr{W}_1$, consists of both a shock and a rarefaction if $\mathbf{c}_m$ and $\mathbf{c}_l$ are on opposite sides of the inflection locus. The shock will always follow the rarefaction in the composed wave, because σ_1 has a maximum along the slow path (Ancona and Marson 2001). Again the order of the waves is reversed in comparison to standard problems such as multi-phase flow in porous media (Juanes and Patzek 2004), because the eigenvalue reflects a retardation rather than a velocity. Figure 3 shows the three possible structures of the slow wave, $\mathscr{W}_1$: (a) rarefaction, $\mathscr{R}_1$, (b) a shock, $\mathscr{S}_1$, (c) shock–rarefaction, $\mathscr{S}_1\mathscr{R}_1$. The figure illustrates how the structure

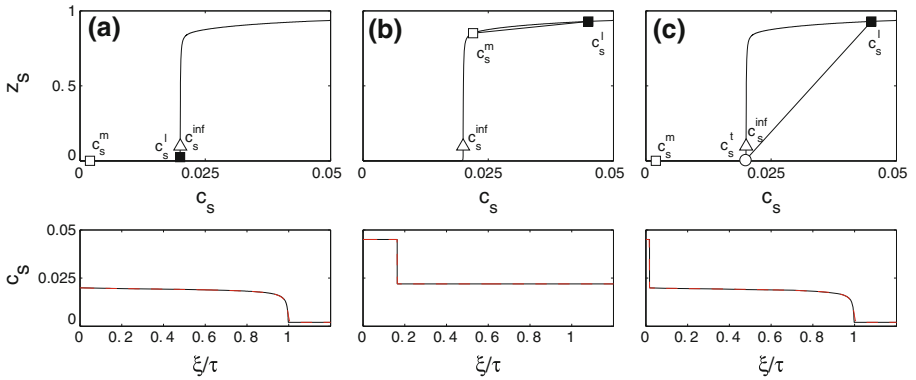

Fig. 3 Structure of the solution along the slow wave $\mathscr{W}_1$ calculated for $c_a = 0.04$. **a** A rarefaction, $\mathscr{R}_1$; **b** a shock, $\mathscr{S}_1$; and **c** a shock–rarefaction, $\mathscr{S}_1\mathscr{R}_1$

of the solution along the slow path is determined by the position of $\mathbf{c}_l$ and $\mathbf{c}_m$ relative to the inflection locus. In the case where both $\mathbf{c}_l$ and $\mathbf{c}_m$ are on the same side of the inflection locus, the isotherm is locally convex and the problem is genuinely nonlinear along the slow path. A rarefaction, $\mathscr{R}_1$, arises when the retardation, σ_1, decreases monotonically from the left to the intermediate state (Fig. 3a). Otherwise a shock, which is a weak solution to the Riemann problem, is introduced to avoid triple valued concentration profiles (Fig. 3b). This genuine shock is physically relevant if it satisfies the Lax entropy condition (Lax 1957)

$$\sigma_1(\mathbf{c}_m) < \tilde{\sigma_1}(\mathbf{c}_m, \mathbf{c}_l) < \sigma_1(\mathbf{c}_l). \tag{40}$$

Finally, a shock–rarefaction arises when $\mathbf{c}_l$ and $\mathbf{c}_m$ lie on the opposite sides of the inflection locus (Fig. 3c) and the problem is not genuinely nonlinear along the slow path (Liu 1974). In our case, as the inflection locus corresponds to the maxima of σ_1 along the slow path the shock is always slower than the rarefaction (Ancona and Marson 2001). A shock–rarefaction corresponds to a shock connecting the left state, $\mathbf{c}_l$, to the tangent point, $\mathbf{c}_t$, such that

$$\tilde{\sigma_1}(\mathbf{c}_l, \mathbf{c}_t) = \sigma_1(\mathbf{c}_t) \tag{41}$$

and a rarefaction connecting $\mathbf{c}_t$ to $\mathbf{c}_m$. The shock must therefore satisfy the Liu entropy condition (Liu 1974; Ancona and Marson 2001) which is an extension of the Lax entropy condition (Eq. 40) which can be written for this system as:

$$\sigma_1(\mathbf{c}_t) \leq \tilde{\sigma_1}(\mathbf{c}, \mathbf{c}_t) < \sigma_1(\mathbf{c}_l), \tag{42}$$

and travels at the speed given by the Rankine–Hugoniot jump condition.

The solution to the Riemann problem with arbitrary $\mathbf{c}_l$ and $\mathbf{c}_r$ is a sequence of two waves $\mathscr{W}_1$ and $\mathscr{W}_2$ and because the problem is linearly degenerate along the fast path there are only three combinations of waves:

Type 1: A rarefaction along the slow path, $\mathscr{R}_1$, and a contact discontinuity along the fast path $\mathscr{C}_2$ (Fig. 4).

Type 2: A shock along the slow path, $\mathscr{S}_1$, and a contact discontinuity along the fast path $\mathscr{C}_2$ (Fig. 5).

Type 3: A shock–rarefaction along the slow path, $\mathscr{S}_1\mathscr{R}_1$, and a contact discontinuity along the fast path $\mathscr{C}_2$ (Fig. 6).

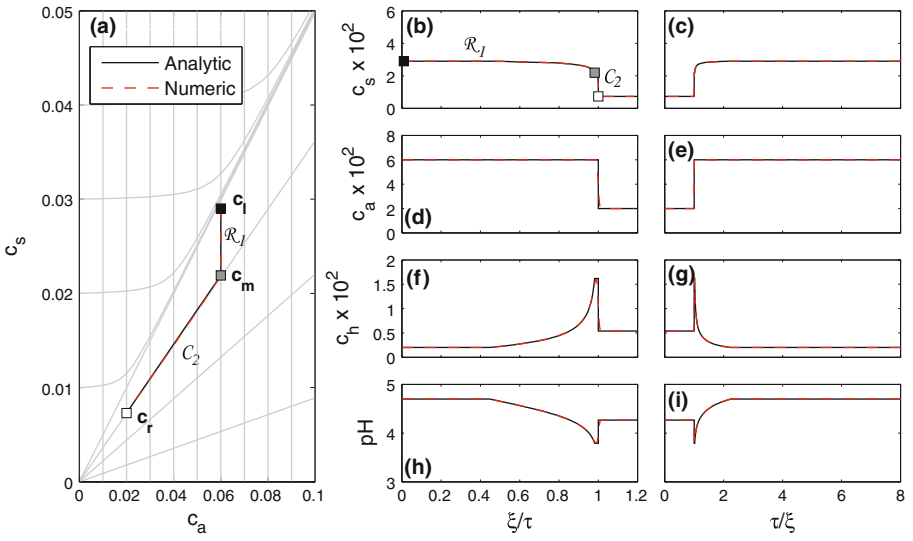

Fig. 4 Composition path, concentration profiles, and breakthrough curves of a Type 1 solution to the Riemann problem. The numerical simulation is with $Pe = 10^5$ and the number of grid points is equal to 50,000. The solution is characterized by a rarefaction along the slow path, $\mathscr{R}_1$, and a contact discontinuity along the fast path, $\mathscr{C}_2$

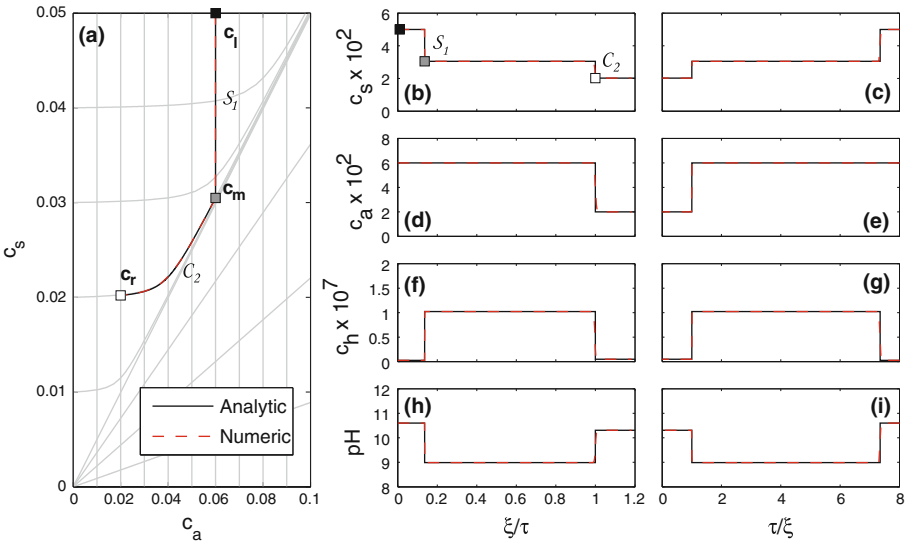

Fig. 5 Composition path, concentration profiles, and breakthrough curves of a Type 2 solution to the Riemann problem. The numerical simulation is with $Pe = 10^5$ and the number of grid points is equal to 50,000. The solution is characterized by a shock along the slow path, $\mathscr{S}_1$, and a contact discontinuity along the fast path, $\mathscr{C}_2$

6 Anomalous Wave

The solution to Eqs. 19 and 20 approaches the physically relevant weak solution of the hyperbolic system of Eq. 24 in the limit of large Pe. This is illustrated throughout the article by the excellent match between highly resolved numerical simulations with negligible numeri-

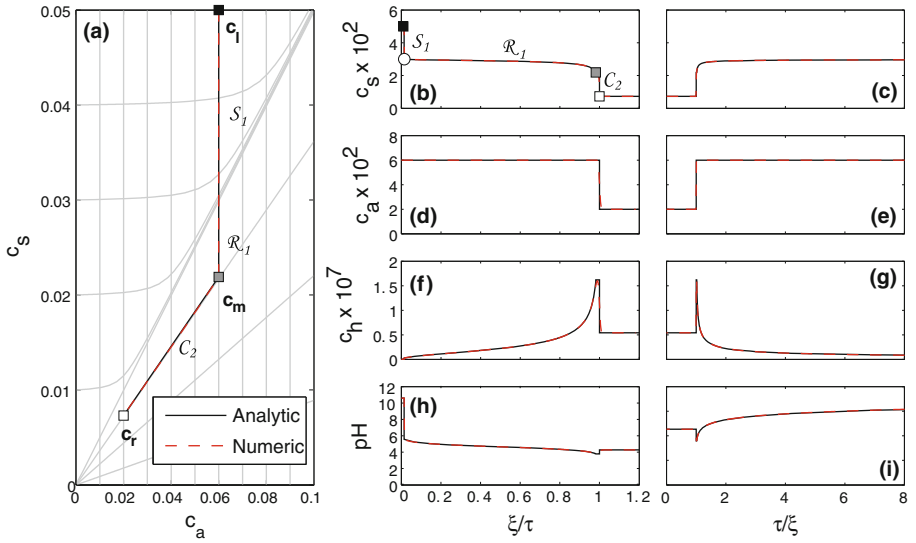

Fig. 6 Composition path, concentration profiles, and breakthrough curves of a Type 3 solution to the Riemann problem. The numerical simulation is with $Pe = 10^5$ and the number of grid points is equal to 50,000. The solution is characterized by a shock–rarefaction along the slow path, $\mathscr{S}_1\mathscr{R}_1$, and a contact discontinuity along the fast path, $\mathscr{C}_2$

cal diffusion and the limiting analytic solution. In the absence of spurious oscillations, the numerical solutions are smoother than the analytic solutions due to the presence of numerical diffusion, which may obscure some wave structures but is not expected to introduce new waves or extrema in the concentration profiles. Therefore, the concentration profiles in Fig. 8 (colored lines) calculated numerically are anomalous in the framework of the theory of chromatography because they present a new wave traveling at the average flow velocity that is not predicted by the theory (black lines). Figure 8 shows three profiles for Type 3 solution, where $c_a^r > c_a^m$, together with the numerical results for $Pe = 10$. In all the three cases, the numerical solution matches the general structure of the analytic solution, but the numerical solution contains an additional wave which is not present in the hyperbolic solution. This wave is a pulse of strontium traveling at the average flow velocity that is superimposed onto the analytic solution.

The anomalous wave is most evident in the case where, $c_s^m = c_s^r = 0$, so that the analytic solution has no structure where the anomalous wave forms, as shown in part d. This is similar to the case studied by Toran et al. (1998) who first reported this behavior in numerical simulations and referred to it as *dual peak behavior*. They identified the interplay of the pH front with the strontium front as the cause for the formation of a fast moving strontium pulse at neutral pH and a retarded strontium front at high pH. Later, Bryant et al. (2000) analyzed the emergence of the wave associated with the pH shock and they showed that dispersion creates a flux of strontium across the pH front where strontium is not adsorbed on the downstream side and therefore forms a *dispersion-induced wave* or *fast wave*. Here, we refer to this phenomenon as anomalous wave or dispersion-induced wave to avoid confusion with the use of the term fast wave in the hyperbolic terminology in Sect. 4.

The emergence of the anomalous wave from a dispersed front is shown in Fig. 7. Part a shows the dispersive mixing zone with the smooth concentration variations between initial

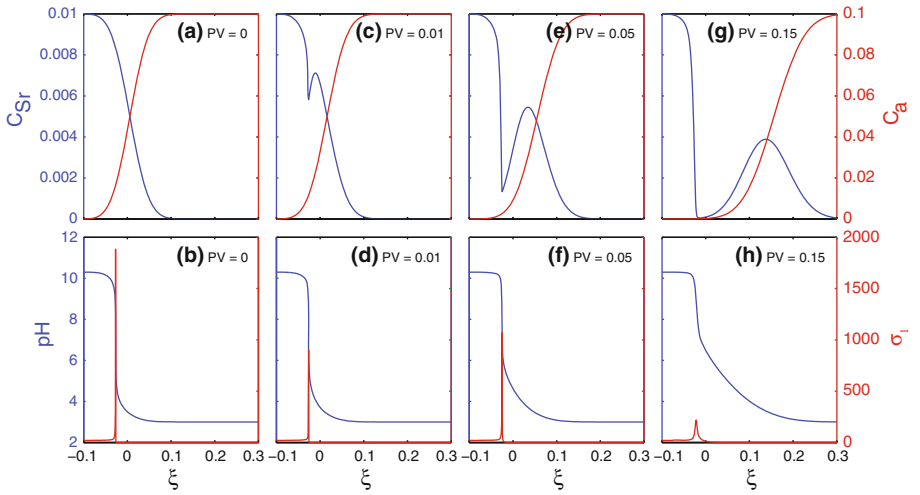

Fig. 7 Emergence of the anomalous wave from a dispersed interface at $Pe = 160$. *Upper figures* report the evolution of the C_{Sr} and the C_{a} concentration profiles; *lower figures* report the corresponding pH profile and the retardation of strontium given by σ_1

and injected states. Part b shows that the pH drops sharply from the injected to the initial value and that most of the mixing zone is at a pH below the sorption edge or equivalently at a strontium concentration below the inflection point of the isotherm as shown in Fig. 1c, b, respectively. Part b also shows the corresponding retardation of strontium, which is given by σ_1. The retardation is negligible throughout the low pH region of the mixing zone, but reaches a pronounced maximum where the pH changes sharply, which corresponds to the strontium concentration at the inflection point. Where the retardation reaches its maximum strong adsorption leads to a local minimum in the strontium concentration profile that eventually separates the retarded front from the anomalous wave which travels downstream at the average flow velocity (part c). Parts e, f show that the anomalous wave is entirely in the region where pH is low and therefore the sorption is negligible and travels together with the effective anion front. In the absence of dispersion, the concentration profile of strontium would have been entirely located upstream of the maximum of the retardation peak while when dispersion is present the concentration front broadens and invades the zone downstream where the retardation is negligible.

The theory of chromatographic established in Sect. 4 has identified the inflection locus and the associated rapid pH change as the key structure in composition space which provides a framework that allows us to define the necessary conditions for the formation of the anomalous wave:

1. A chromatographic system with a competitive Langmuir isotherm of sigmoidal shape.
2. The injection composition, $\mathbf{c}_{\mathrm{I}}$, above the inflection locus and the initial condition, $\mathbf{c}_{\mathrm{r}}$, below it, so that the slow wave, $\mathscr{W}_1$, crosses the inflection locus in the hodograph plane.
3. The effective anion concentration in the injection composition, $c_{\mathrm{a}}^{\mathrm{I}}$, smaller than in the initial composition, $c_{\mathrm{a}}^{\mathrm{r}}$, so that c_{a} increases across the fast wave, $\mathscr{W}_2$.
4. A physical system with a finite amount of dispersion, $Pe < \infty$.

A comparison of the path in the hodograph plane in Fig. 8a and the pH contours in Fig. 1d shows that the third necessary condition implies that the pH decreases from $\mathbf{c}_{\mathrm{m}}$ to $\mathbf{c}_{\mathrm{r}}$ along

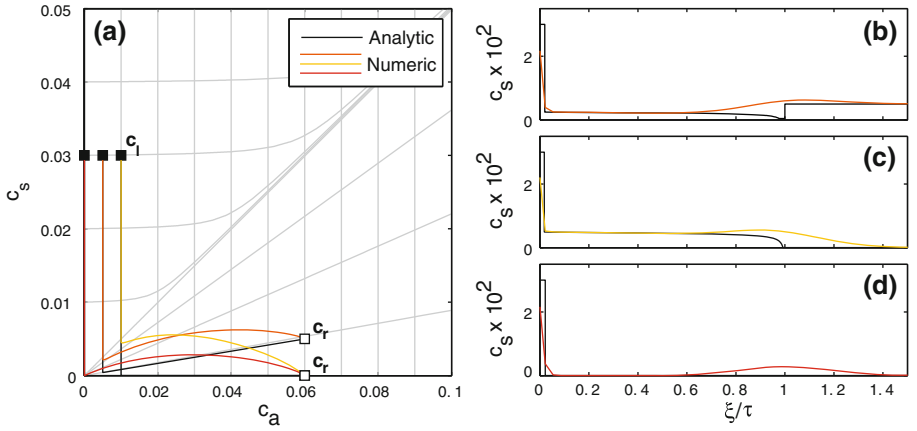

Fig. 8 Three examples of Type 3 solution in the presence of the anomalous wave. Numerical solutions are with $Pe = 10^3$ and number of grid points equal to 2,000, and a slightly broadened initial condition to emphasize the anomalous wave

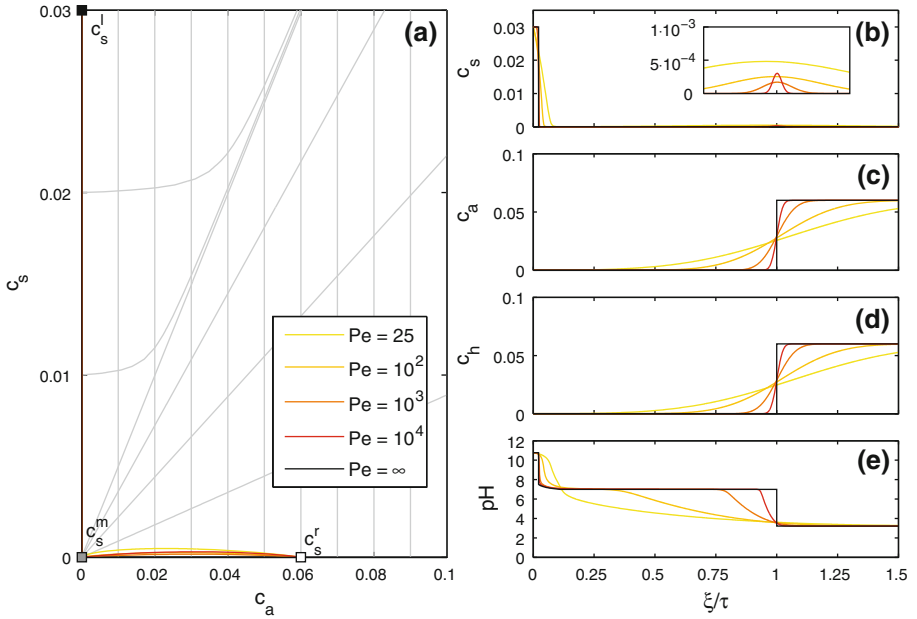

Fig. 9 Analysis of the effect of Pe on the magnitude of the anomalous wave. In contrast to Fig. 8, the initial condition here is a step hence the reduced amplitude of the anomalous wave

$\mathscr{W}_2$. Therefore, in the presence of hydrodynamic dispersion (fourth necessary condition) the initial discontinuity instantaneously broadens so that strontium is also present downstream of the initial step in the region of low pH and therefore negligible adsorption. In the case of the analytical solution to the Riemann problem in the absence of dispersion, the strontium front always travels with the pH front and is therefore strongly retarded.

The most evident anomalous wave obtained in the case of $c_s^m = c_s^r = 0$ (Fig. 8d) is further analyzed under increasing Pe in Fig. 9. Part a of this figure shows how the deflection of

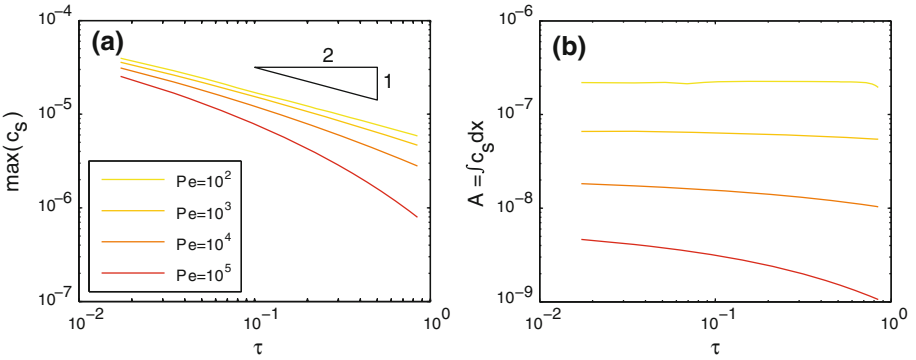

Fig. 10 Evolution of the magnitude of the pulse of the anomalous wave for different Pe. **a** Height of the pulse and **b** area under the pulse

the composition path from the analytic solution in the hodograph plane also increases with decreasing Pe. While, part b shows the increase of the volume and width of the wave with decreasing Pe, but the amplitude of the anomalous wave is not a monotonic function of Pe.

Finally, Fig. 10 shows the temporal evolution of the wave for different Pe. At small Pe, the amplitude of the anomalous wave decays as $1/\sqrt{t}$ and the area of the wave is approximately constant. This indicates that the anomalous wave at low Pe decays mostly due to hydrodynamic dispersion and that the adsorption is negligible. At high Pe, the amplitude of the anomalous wave decays faster than $1/\sqrt{t}$ and the area of the wave decays slowly. This indicates that the smaller anomalous waves, which form at high Pe, decay due to adsorption. The loss occurs at the tail of the dispersive wave where a decrease in c_a and an increase in pH lead to adsorption.

7 Conclusions

In this study, we have analyzed the reactive transport problem of an aqueous system with competitive adsorption of strontium and hydrogen in the presence of sodium and chlorine. Unlike the competitive adsorption between two metals that leads to a concave Langmuir isotherm, the nonlinearity of the dissociation of hydrogen leads to a competitive Langmuir isotherm with an inflection point. The reactive transport model is reduced to a 2×2 system of conservation laws for strontium and an effective anion which in the absence of dispersion is strictly hyperbolic and can be analyzed in the framework of the theory of chromatography.

The full set of solutions to the Riemann problem comprises two waves connected by an intermediate composition. The fast wave is a contact discontinuity traveling at the average flow velocity while the slow wave may either be a shock, a rarefaction, or a shock–rarefaction. The shock–rarefaction arises due to the sigmoidal shape of the isotherm and does not arise in systems with a concave Langmuir isotherm. Numerical solutions with very high Péclet numbers show excellent agreement with the analytic solutions in the hyperbolic limit. In the presence of hydrodynamic dispersion, a pulse forms in the strontium profile if the slow wave crosses the inflection point and the effective anion concentration increases along the fast path. Given the full set of solutions to the Riemann problem in the limit of no dispersion this wave is anomalous, because is not predicted by the theory of chromatography. This anomalous wave is in the form of a pulse of strontium traveling at the average flow velocity

superimposed onto the fast wave. It forms because dispersion instantaneously broadens the initial discontinuity so that strontium is also present downstream of the initial step in the region of negligible adsorption, therefore also the name of dispersion-induced wave.

Acknowledgments This material is based upon work supported as part of the Center for Frontiers of Subsurface Energy Security (CFSES), an Energy Frontier Research Center funded by the US Department of Energy, Office of Science, Office of Basic Energy Sciences under Award Number DE-SC0001114. Acknowledgment is made to the Donors of the American Chemical Society Petroleum Research Fund, for partial support of this research.

Appendix: Numerical Discretization

A finite volume scheme was developed to discretize the nonlinear system of Eqs. 21 and 22. The accumulation term is not expanded, but differenced directly to treat the nonlinearity implicity. The advection term is integrated explicitly and approximated with an upwind flux, while the hydrodynamic dispersion term is integrated implicity and approximated by a central flux (LeVeque 2008). The domain, $\xi \in [0,\ 1]$, is divided into a grid with $N+2$ cells, where all interior cells are of width $\Delta\xi = 1/(N+1)$ and the two boundary cells are of width $\Delta\xi/2$. The cell centers are located at $\xi_i = (i-1)\Delta\xi$ for $i \in [0, N+1]$ and the numerical solution in the ith cell is denoted $c_{\mathrm{s},i}$ and $c_{\mathrm{a},i}$. The discretization in the interior cells, $1 \le i \le N$, at time τ_n is given by

$$\frac{(c_\mathrm{s}+\phi z_\mathrm{s})_i^{n+1}-(c_\mathrm{s}-\phi z_\mathrm{s})_i^{n}}{\Delta\tau}+\frac{c_{\mathrm{s},i}^{n}-c_{\mathrm{s},i-1}^{n}}{\Delta\xi}-\frac{1}{Pe}\frac{c_{\mathrm{s},i+1}^{n+1}-2c_{\mathrm{s},i}^{n+1}+c_{\mathrm{s},i-1}^{n+1}}{\Delta\xi^2}=0, \quad (43)$$

$$\frac{c_{\mathrm{a},i}^{n+1}-c_{\mathrm{a},i}^{n}}{\Delta\tau}+\frac{c_{\mathrm{a},i}^{n}-c_{\mathrm{a},i-1}^{n}}{\Delta\xi}-\frac{1}{Pe}\frac{c_{\mathrm{a},i+1}^{n+1}-2c_{\mathrm{a},i}^{n+1}+c_{\mathrm{a},i-1}^{n+1}}{\Delta\xi^2}=0. \quad (44)$$

The resulting nonlinear algebraic system of $2N$ equations is solved with the Newton–Raphson method and the timestep is chosen adaptively based on the convergence of the Newton iteration with a maximum time step given by the CFL condition (Aziz and Settari 2002). The accuracy of this discretization is tested in Sect. 5 by comparison against the analytic solution. For the convergence of the numerical solution towards the hyperbolic solution, in the limit of $Pe \gg 1$, up to $N = 50{,}000$ grid points are necessary. In this case, we eliminate the dispersion term entirely and the resulting diagonal Jacobian matrix allows efficient solution of the Newton iterations for large N.

References

Ancona, F., Marson, A.: A note on the Riemann problem for general $n \times n$ conservation laws. J. Math. Anal. Appl. **260**(1), 279–293 (2001). doi:10.1006/jmaa.2000.6721

Appelo, C.: Multicomponent ion exchange and chromatography in natural systems. In: Lichtner P.C., Steefel C. I., Oelkers E. H. (eds.) Reactive Transport in Porous Media, Reviews in Mineralogy, Vol. 34, pp. 193–227. Mineralogical Society of America (1996) Short Course on Reactive Transport in Porous Media, Golden, CO, Oct 25–27, 1996

Appelo, C., Hendriks, J., Van Veldhuizen, M.: Flushing factors and a sharp front solution for solute transport with multicomponent ion-exchange. J. Hydrol. **146**(1–4), 89–113 (1993). doi:10.1016/0022-1694(93)90271-A

Aziz, K., Settari, T.: Petroleum Reservoir Simulation. Blitzprint Ltd., Calgary (2002)

Bankston, T.E., Dattolo, L., Carta, G.: pH Transients in hydroxyapatite chromatography columns—experimental evidence and phenomenological modeling. J. Chromatogr. A **1217**(14), 2123–2131 (2010). doi:10.1016/j.chroma.2010.02.004

Berkowitz, B., Cortis, A., Dentz, M., Scher, H.: Modeling non-Fickian transport in geological formations as a continuous time random walk. Rev. Geophys. **44**(2) (2006). doi:10.1029/2005RG000178

Bryant, S., Dawson, C., van Duijn, C.: Dispersion-induced chromatographic waves. Ind. Eng. Chem. Res. **39**(8), 2682–2691 (2000). doi:10.1021/ie990796e

Cantwell, B. : Introduction to Symmetry Analysis. Vol. II, Cambridge University Press, Cambridge (2002)

Charbeneau, R.: Groundwater contaminant transport with adsorption and ion-exchange chemistry—method of characteristics for the case without dispersion. Water Resour. Res. **17**(3), 705–713 (1981). doi:10.1029/WR017i003p00705

Charbeneau, R.: Multicomponent exchange and subsurface solute transport—characteristics, coherence, and the Riemann problem. Water Resour. Res. **24**(1), 57–64 (1988). doi:10.1029/WR024i001p00057

Das, S., Hendry, M.J., Essilfie-Dughan, J.: Transformation of two-line ferrihydrite to goethite and hematite as a function of pH and temperature. Environ. Sci. Technol. **45**(1), 268–275 (2011). doi:10.1021/es101903y

Dattolo, L., Keller, E.L., Carta, G.: pH Transients in hydroxyapatite chromatography columns—effects of operating conditions and media properties. J. Chromatogr. A **1217**(48), 7573–7578 (2010). doi:10.1016/j.chroma.2010.10.026

Glueckauf, E.: Theory of chromatography; chromatograms of a single solute. J. Chem. Soc. 1302–1308 (1947). doi:10.1039/jr9470001302

Greskowiak, J., Hay, M., Prommer, H., Liu, C., Pos, V., Ma, R., Davis, J., Zheng, C., Zachara, J.: Simulating adsorption of U(VI) under transient groundwater flow and hydrochemistry: physical versus chemical nonequilibrium model. Water Resour. Res. **47**, 403–409 (2011). doi:10.1029/2010WR010118

Haggerty, R., Gorelick, S.: Multiple-rate mass-transfer for modeling diffusion and surface-reactions in media with pore-scale heterogeneity. Water Resour. Res. **31**(10), 2383–2400 (1995). doi:10.1029/95WR10583

Helfferich, F., Klein, G.: Multicomponent Chromatography. Marcel Dekker, New York (1970)

Hiemstra, T., Van Riemsdijk, W.: A surface structural approach to ion adsorption: the charge distribution (CD) model. J. Colloid Interface Sci. **179**(2), 488–508 (1996). doi:10.1006/jcis.1996.0242

Hiemstra, T., Dewit, J., Van Riemsdijk, W.: Multisite proton adsorption modeling at the solid–solution interface of (hydr)oxides—a new approach. II. Application to various important (hydr)oxides. J. Colloid Interface Sci. **133**(1), 105–117 (1989). doi:10.1016/0021-9797(89)90285-3

Hiemstra, T., Rahnemaie, R., Van Riemsdijk, W.: Surface complexation of carbonate on goethite: IR spectroscopy, structure and charge distribution. J. Colloid Interface Sci. **278**(2), 282–290 (2004). doi:10.1016/j.jcis.2004.06.014

Juanes, R., Patzek, T.: Analytical solution to the Riemann problem of three-phase flow in porous media. Transp. Porous Media **55**(1), 47–70 (2004). doi:10.1023/B:TIPM.0000007316.43871.1e

Knapp, R.: Spatial and temporal scales of local equilibrium in dynamic fluid-rock systems. Geochim. Cosmochim. Acta **53**(8), 1955–1964 (1989). doi:10.1016/0016-7037(89)90316-5

Lake, L., Bryant, S., Araque-Martinez, A.: Geochemistry and Fluid Flow. 1st edn. Elsevier, Amsterdam (2002)

Lax, P.: Hyperbolic systems of conservation laws, II. Commun. Pure Appl. Math. **10**, 537–566 (1957)

LeVeque, R.J.: Numerical Methods for Conservation Laws. 2nd edn. Birkhäuser, Berlin (2008)

Liu, T.: Riemann problem for general 2×2 conservation laws. Trans. Am. Math. Soc. **199**, 89–112 (1974)

Mazzotti, M.: Local equilibrium theory for the binary chromatography of species subject to a generalized Langmuir isotherm. Ind. Eng. Chem. Res. **45**(15), 5332–5350 (2006). doi:10.1021/ie060297v

Orr, F.J. : Theory of Gas Injection Processes. Vol. II, Tie-Line Publications, Holte (2007)

Pabst T.M., Carta G.: pH Transitions in cation exchange chromatographic columns containing weak acid groups. J. Chromatogr. A **1142**(1), 19–31 (2007). doi:10.1016/j.chroma.2006.08.066. 19th International Symposium on Preparative and Process Chromatography, Baltimore, MD, May 14–17, 2006

Pope, G., Lake, L., Helfferich, F.: Cation-exchange in chemical flooding. I. Basic theory without dispersion. Soc. Pet. Eng. J. **18**(6), 418–434 (1978)

Rhee, H., Amundson, N.: Study of shock layer in nonequilibrium exchange systems. Chem. Eng. Sci. **27**(2), 199 (1972). doi:10.1016/0009-2509(72)85057-7

Rhee, H., Bodin, B.F., Amundson, N.: Study of the shock layer in equilibrium exchange systems. Chem. Eng. Sci. **26**, 1571–1580 (1971)

Rhee, H.K., Aris, A., Amudson, N. : First-Order Partial Differential Equations, Theory and Application of Hyperbolic Systems of Quasilinear Equations. Vol. II, Prentice-Hall, Englewood Cliffs, NJ (1989)

Saunders, J., Toran, L.: Modeling of radionuclide and heavy metal sorption around low- and high-pH waste disposal sites at Oak Ridge, Tennessee. Appl. Geochem. **10**(6), 673–684 (1995). doi:10.1016/0883-2927(95)00036-4

Scher, H., Margolin, G., Berkowitz, B.: Towards a unified framework for anomalous transport in heterogeneous media. Chem. Phys. **284**(1–2, SI), 349–359 (2002). doi:10.1016/S0301-0104(02)00558-X

Spalding, B., Spalding, I.: Chemical equilibria model of strontium-90 adsorption and transport in soil in response to dynamic alkaline conditions. Environ. Sci. Technol. **35**(2), 365–373 (2001). doi:10.1021/es001445q

Temple, B.: Systems of conservation laws with coinciding shock and rarefaction curves. Contemp. Math. **17**, 143–151 (1983)

Toran, L., Bryant, S., Saunders, J., Wheeler, M.: A two-tiered approach to reactive transport: application to Sr mobility under variable pH. Ground Water **36**(3), 404–408 (1998). doi:10.1111/j.1745-6584.1998.tb02810.x

US EPA. Radiation Protection. Strontium: http://epa.gov/radiation/radionuclides/strontium.html (2011)

Valocchi, A., Street, R., Roberts, P.: Transport of ion-exchanging solutes in groundwater—chromatographic theory and field simulation. Water Resour. Res. **17**(5), 1517–1527 (1981). doi:10.1029/WR017i005p01517

van Beinum, W., Hofmann, A., Meeussen, J., Kretzschmar, R.: Sorption kinetics of strontium in porous hydrous ferric oxide aggregates I. The Donnan diffusion model. J. Colloid Interface Sci. **283**(1), 18–28 (2005). doi:10.1016/j.jcis.2004.08.067

Wieland, E., Tits, J., Kunz, D., Daehn, R.: Strontium uptake by cementitious materials. Environ. Sci. Technol. **42**(2), 403–409 (2008). doi:10.1021/es071227y

Zhu, C., Schwartz, F.W.: Hydrogeochemical processes and controls on water quality and water management. Elements **7**(3), 169–174 (2011). doi:10.2113/gselements.7.3.169